https://ntrs.nasa.gov/search.jsp?R=19960038141 2020-06-16T04:28:39+00:00Z

NASA-TM-111707

TN-39-TM
6762

JSC 25685

c.383

Stress Intensity Factors for Part-through Surface Cracks in Hollow Cylinders

Structures and Mechanics Division

July 1992

LESC 30124

U.S. Gov't

LIBRARY
Center
Texas 77058

Stress Intensity Factors for Part-through Surface Cracks in Hollow Cylinders

JOB ORDER 85-130

Prepared by:

Sambi R. Mettu
Adv. Systems Engineering Specialist
Lockheed Engineering & Sciences Co.,

Ivatury S. Raju
Senior Scientist
Analytical Services & Materials Inc.,

Concurrence:

Lockheed ESC

V. Shivakumar
Adv. Systems Engineering Specialist
Engineering Software Systems Section

James F. Brose
Supervisor,
Engineering Software Systems Section

NASA/JSC

Royce G. Forman
Senior Materials Engineer
Metallic Materials Section

Willard L. Castner
Head, Metallic Materials Section

Approved by:

John H. Knesek
Manager, Materials & Engineering
Software Systems Department

Lubert J. Leger
Chief, Materials Branch

U.S. Gov't

JSC 25685
LESC 30124

Stress Intensity Factors for Part-Through Surface Cracks in Hollow Cylinders

Sambi R. Mettu
Lockheed Engineering & Sciences Company
Ivatury S. Raju
Analytical Services & Materials Inc.,
and
Royce G. Forman
NASA Lyndon B. Johnson Space Center

Abstract

Flaws resulting from improper welding and forging are usually modeled as cracks in flat plates, hollow cylinders or spheres. The stress intensity factor solutions for these crack cases are of great practical interest. This report describes some recent efforts at improving the stress intensity factor solutions for cracks in such geometries with emphasis on hollow cylinders. Specifically, two crack configurations for cylinders are documented. One is that of a surface crack in an axial plane and the other is a part-through thumb-nail crack in a circumferential plane. The case of a part-through surface crack in flat plates is used as a limiting case for very thin cylinders. A combination of the two cases for cylinders is used to derive a relation for the case of a surface crack in a sphere. Solutions were sought which cover the entire range of the geometrical parameters such as cylinder thickness, crack aspect ratio and crack depth. Both the internal and external position of the cracks are considered for cylinders and spheres. The finite element method was employed to obtain the basic solutions. Power-law form of loading was applied in the case of flat plates and axial cracks in cylinders and uniform tension and bending loads were applied in the case of circumferential (thumb-nail) cracks in cylinders. In the case of axial cracks, the results for tensile and bending loads were used as reference solutions in a weight function scheme so that the stress intensity factors could be computed for arbitrary stress gradients in the thickness direction. For circumferential cracks, since the crack front is not straight, the above technique could not be used. Hence for this case, only the tension and bending solutions are available at this time. The stress intensity factors from the finite element method were tabulated so that results for various geometric parameters such as crack depth-to-thickness ratio(a/t), crack aspect ratio(a/c) and internal radius-to-thickness ratio(R/t) or the crack length- to-width ratio ($2c/W$) could be obtained by interpolation and extrapolation. Such complete tables were then incorporated into the NASA/FLAGRO computer program which is widely used by the aerospace community for fracture mechanics analysis.

U.S. Gov't

Introduction

Flaws resulting from improper welding and forging are usually modeled as cracks in flat plates, hollow cylinders or spheres. In real structures, in addition to through cracks, a common type of flaw that occurs is the part-through type. Pressure vessels and pipes are vital components in many engineering systems. These may be modeled as cylinders or spheres depending on the geometry. Among space applications, the Space Shuttle and Space Station Freedom contain many pressure vessels and lines containing hazardous or nonhazardous fluids whose failure will either be catastrophic or lead to aborting the mission. Fracture mechanics methods are necessary to assess the structural integrity of such components. The stress intensity factor solution is an essential element in fracture mechanics analysis. It is desirable to be able to deal with nonuniform stress gradients in such important configurations. Towards this goal, work was initiated to obtain finite element solutions of these crack configurations covering a wide range of geometrical parameters.

This report describes some recent efforts at improving the stress intensity factor solutions for the geometries mentioned above. Specifically, two crack configurations for cylinders are documented. One is that of a surface crack in an axial plane and the other is a part-through thumb-nail crack in a circumferential plane. The case of a part-through surface crack in flat plates is used as a limiting case for very thin cylinders. A combination of the two cases for cylinders is used to derive a relation for the case of a surface crack in a sphere. Fig. 1 shows the cases of a flat plate and a sphere having surface cracks. These were denoted as crack cases SC02 and SC03 respectively in NASA/FLAGRO[1, 2]. Fig. 2 shows the two crack cases for cylinders denoted as SC04 and SC05. Solutions were sought which cover the entire range of the geometrical parameters such as cylinder thickness, crack aspect ratio and crack depth. Both the internal and external position of the cracks were considered for cylinders and spheres. The finite element method was employed to obtain the basic solutions. Power-law form of loading was applied in the case of axial cracks and uniform tension and bending loads were applied in the case of circumferential (thumb-nail) cracks. In the case of axial cracks, the results for tensile and bending loads were used as reference solutions in a weight function scheme so that the stress intensity factors could be computed for arbitrary stress gradients in the thickness direction. For circumferential cracks, since the crack front is not straight, the above technique could not be used. Hence for this case, only the tension and bending solutions are possible at this time. In all cases, the stress intensity factors from the finite element method were tabulated so that results for various geometric parameters such as crack depth-to-thickness ratio(a/t), crack aspect ratio(a/c) and internal radius-to-thickness ratio(R/t) or crack length-to-width ratio($2c/W$) could be obtained by interpolation and extrapolation. Such complete tables were then

U.S. Gov't

incorporated into the NASA/FLAGRO computer program which is widely used by the aerospace community for fracture mechanics analysis.

The raw data from finite element analysis was presented in a report by Raju[3]. A demonstration of the accuracy of the weight function method in dealing with nonuniform stresses was presented by Forman et. al.[4] for the case of axial cracks in hollow cylinders. Results published earlier by Raju and Newman[5] for $R/t = 4$ and 10 were used in that study. The recently obtained results for $R/t = 1$ and 2, and their weight function implementation are included in the present report. Similar results for the case of flat plates with surface cracks were documented in Ref. [6] by Raju et. al. For the sake of completeness, the present report includes the results for all the fractional-power loads in the case of a surface crack in a flat plate and axial cracks in cylinders, even though only the results for integer-power loads were used for implementing and verifying the weight function method.

Solutions using Finite Element Method

The finite element method(FEM) is versatile enough to be used in generating any desired stress intensity factor solution. The limitation is the need for extensive computing resources and the resulting inefficiency in solving a given geometrical configuration, especially in the context of fatigue crack growth analysis where solutions are needed for many different crack lengths. It is more efficient first to develop the solutions for certain discrete values of the geometrical parameters spanning their complete possible range and then to use tabular interpolation and extrapolation for specific values of the parameters. This is the approach adopted in the present work. The modeling and computing of the stress intensity factors for the case of an axial crack in a cylinder(SC04) was first undertaken by Raju and Newman[5]. They developed the finite element models and obtained solutions for two values of the ratio of internal radius to thickness ($R/t = 4$ and 10). The nondimensional stress intensity correction factors(SICF) defined by $F_p = K/\sigma_0\sqrt{\pi a/Q}$ where $Q = 1 + 1.464(a/c)^{1.65}$ for $a/c \leq 1$ and $Q = 1 + 1.464(c/a)^{1.65}$ for $a/c > 1$ were obtained for internal and external cracks. Results for two points along the crack front, the surface point(c–tip) and the deepest point(a–tip), were listed. Singular elements were used near the crack tip and a force method was used to extract the stress intensity factors. Figs. 1 and 2 shows the coordinate system used. x is the distance measured along the thickness direction starting at the crack mouth. Loading of the form $\sigma_0(x/a)^n$ was considered where $n = 0$, 1, 2 and 3. Fig. 3 shows these loads which are applied only on the crack face. Power $n = 0$ corresponds to uniform tension and power $n = 1$ gives a linear distribution from which the case of bending can be derived.

Recently Raju[3] obtained the complete set of results for $R/t = 1$ and 2 for loads with $n = 0$, .5, 1, 1.5, 2, 2.5, 3 and 3.5 across the crack face. Thus, results for the full range of

U.S. Gov't

R/t = 1.0, 2.0, 4.0 and 10.0 are now available for all the integer powers. The results from a flat plate solution can be used for a large value of R/t = 300.0. The FEM solutions were obtained for crack aspect ratios a/c of 0.2, .4 and 1.0. Also, crack-depth ratios a/t were set to 0.2, 0.5, and 0.8. Results for both internal and external positioning of the crack were obtained at several locations along the crack front including the surface point(c–tip) and deepest point(a–tip). Tables 1 to 8 list all the available results for this crack case SC04. For the sake of convenient reference, the results from Ref. [5] are also included in the present tables. Tables 1 to 4 list the values for integer powers n = 0, 1, 2 and 3. The new results for R/t = 1 and 2 for powers 0.5, 1.5, 2.5 and 3.5 are listed in Tables 5 to 8. It may be noted that in all the tables, the results for R/t = 300 are those for flat plates reported in Ref. [3]. This full set of results is operated upon by standard Hermite type of interpolation/extrapolation to obtain the results for an arbitrary geometry. This set of results was then used in the weight function method described briefly next. In the tables, the values listed for the two crack-depth-to thickness ratios(a/t =0 and 1.0) are obtained by smooth extrapolation using a Hermite type fit for each a/c. The results were plotted to ensure smoothness of the interpolation and extrapolation.

For the case of a circumferential thumb-nail crack, the results were obtained for tension and bending loads only. These are listed in Tables 9 and 10. The SIF correction factors in these two tables are defined differently. Factors $F_0 = K/\sigma_0\sqrt{\pi a}$ are shown. Here also, the extrapolated values for a/t = 0 and 1 are shown in the tables. Good finite element solutions could not be obtained for low aspect ratios (a/c = 0.2 and 0.4) because of distortion of the elements; hence extrapolation was used to obtain results for a/c = 0.2, 0.4 and 2.0. Fig. 4 shows an example of such a distorted mesh.

Finally, the stress intensity factor solutions for the case of a surface crack in a sphere (SC03) were constructed using a combination of the solutions of the axial and circumferential cracks in cylinders(SC04 and SC05). The empirical equation which combines the two solutions is as follows:

$$F_3 = F_2(F_4/F_2)(F_5/F_2) \tag{1}$$

where the subscript on the stress intensity correction factors indicates the crack case number. This is assumed to hold good only for tensile loading. The two ratios on the right hand side are thought of as corrections to the flat plate solution, to account for the curvature of the sphere. The flat plate solution F_2 used here is based on a small value of the ratio $2c/W$. For bending loading, the solution is assumed to be same as that of a flat plate.

U.S. Gov't

Solutions using Weight Function Method

The weight function(WF) method was conceived by Bueckner[7] and Rice[8] and was used by several investigators to generalize the stress intensity factor solutions for cracks subjected to arbitrary loading. For one-dimensional variation of stresses acting across the potential crack plane, the basic relation between the stress intensity factor and the stress distribution is given by

$$K_r = \int_0^a \sigma_r(x) m(x,a) dx \tag{2}$$

where $\sigma_r(x)$ is the stress distribution on the crack face and $m(x,a)$ is the weight function which varies with the position coordinate x and the crack length a. Once the weight function is known, the stress intensity factor can be obtained by numerical quadrature. Variations in implementing the weight function scheme are essentially in the way the function $m(x,a)$ is obtained. It can be shown that

$$m(x,a) = \frac{H}{K} \frac{\partial u(x,a)}{\partial a} \tag{3}$$

where the stress intensity factor K and the crack face displacement $u(x,a)$ correspond to the same applied loading. H is a material constant and a is the crack length.

A new approach to computing the weight function was proposed by Shen and Glinka[9, 10]. In their approach, the weight function is assumed to be a four-term approximation in the form

$$m(x,a) = \frac{2}{\sqrt{2\pi(a-x)}} \left(1 + M_1(1-\frac{x}{a})^{1/2} + M_2(1-\frac{x}{a}) + M_3(1-\frac{x}{a})^{3/2}\right) \tag{4}$$

where the crack tip is at $x = a$. In principle, the three constants M_1, M_2, M_3 can be determined from three reference solutions for the stress intensity factors and there would be no need to obtain the displacement field. Thus, the inaccuracies resulting from numerical differentiation of the displacement field are avoided. The novelty of the present method is in going another step forward by direct and accurate usage of numerical reference solutions in tabular form as opposed to using reference solutions in analytical form. In Ref. [6] this method was implemented for surface cracks in flat plates using reference solutions based on recent finite element solutions for various stress distributions on the crack face and their tabular interpolation. In Ref. [4] this approach was extended to the case of axial part-through cracks in hollow cylinders. The weight functions for the axial surface crack in hollow cylinders is assumed to be of the same form as in flat plates. The effects of curvature are brought in by the reference solutions. Otherwise, the scheme is identical to that of flat plates. The weight functions are given for the surface point or c–tip in our notation by

$$m_B(x,a) = \frac{2}{\sqrt{\pi x}} \left(1 + M_{1B}(\frac{x}{a})^{1/2} + M_{2B}(\frac{x}{a}) + M_{3B}(\frac{x}{a})^{3/2}\right) \tag{5}$$

U.S. Gov't

and for the deepest point or a–tip, by

$$m_A(x,a) = \frac{2}{\sqrt{2\pi(a-x)}}\left(1 + M_{1A}(1-\frac{x}{a})^{1/2} + M_{2A}(1-\frac{x}{a}) + M_{3A}(1-\frac{x}{a})^{3/2}\right) \quad (6).$$

In order to solve for the three constants in each of the above two equations, two reference solutions and a third condition are used. As explained in Ref. [10], the third condition for the c–tip is that the weight function vanishes at $x = a$ which gives

$$1 + M_{1B} + M_{2B} + M_{3B} = 0 \quad (7)$$

and the third condition for the a–tip is that the second derivative of the weight function be zero at x =0 leading to

$$M_{2A} = 3 \quad (8).$$

The two reference solutions used are the case of uniform tension and linearly decreasing stress as illustrated in Fig. 5 and the correction factors for the stress intensity are those from Tables 1 to 2. The solution for linearly decreasing stress is given by $F_2 = F_U - F_L$ where F_U is for uniform loading(n =0) and F_L is for linearly increasing loading(n =1).

Figs. 6 to 13 show a comparison of the results from the weight function method with those obtained using finite elements for various distributions of stresses for the cases of internal or external axial cracks in hollow cylinders. The symbols denote the FEM results and the curves indicate the computed weight function solutions. The good agreement of finite element data with the weight function results indicates self-consistency and accuracy of numerical integration for both the c–tip and the a–tip for n =0, 1, 2 and 3. These results establish that the assumed weight function works for the cylinders as well. NASA/FLAGRO can be used to compute the stress intensity factors for any specified geometry. In the present set of results, a crack aspect ratio of a/c =1 was used.

Discussion

As mentioned earlier, for crack case SC04, only the results for tension and linear loads as listed in Tables 1 and 2 are used as reference solutions in the weight function method. The results in Tables 3 and 4 were compared with independently computed values from weight function routines. These comparisons are shown in Figs. 6 to 13 and excellent agreement of the weight function results with those from finite elements for all powers n =0, 1, 2, and 3, is seen, thus indicating the accuracy of the method. The value of a/c =1 was used in these comparisons. Equally good agreement was observed for other values of a/c ranging from 0.1 to 2.0. As demonstrated in Ref.[6], weight function method gives accurate solutions for flat plates also. The empirical equation for the case of a sphere

U.S. Gov't

presented earlier is based on intuition alone and will have to be verified in future using finite element or other methods.

Summary and Conclusions

Four crack configurations developed for fracture control of space hardware which may be modeled as flat plates, cylinders or spheres are shown and their stress intensity factor solutions are presented. Efforts to improve the stress intensity factor solutions for these cases to account for general loading based on the weight function method are described. Specifically, solutions for the cases of a part-through axial or a part-through thumb-nail crack on either the inside or the outside of the cylinders or in a flat plate were considered. Numerical finite element solutions of stress intensity factors for the whole array of geometrical parameters were tabulated and a standard Hermite type of interpolation scheme was used so that the stress intensity factors can be obtained for arbitrary geometries. Solutions for the reference loading cases of constant and linearly varying stresses were used in a weight function approach and comparisons were made with the FEM solutions for higher order loading. The excellent agreement establishes the accuracy of the method. An empirical solution was constructed for the case of a surface crack in a sphere using the solutions for hollow cylinders and flat plates.

Acknowledgements

The authors appreciate the efforts of Drs. T. Krishnamurthy and K.N. Shivakumar of Analytical Services and Materials Inc.(AS & M) in providing the stress intensity factor solutions using three dimensional finite element analysis. Valuable discussions with Dr. V. Shivakumar of Lockheed Engineering & Sciences(LESC) are appreciated. The effort of Mr. F. Yeh of LESC in preparing the figures is also gratefully acknowledged. Support under contracts NAS1-19317 from NASA Langley to AS & M and NAS9-17900 from NASA JSC to LESC was provided during the course of this work.

U.S. Gov't

References

[1] Forman, R.G., Shivakumar, V., Newman, J.C. Jr., Piotrowski, S.M., and Williams, L.C., "Development of the NASA/FLAGRO Computer Program," Fracture Mechanics: Eighteenth Symposium, ASTM STP 945, D.T. Read and R.P. Reed, Eds., American Society for Testing and Materials, Philadelphia, 1988, pp. 781-803.

[2] "Fatigue Crack Growth Computer Program, NASA/FLAGRO" JSC-22267, NASA Lyndon B. Johnson Space Center, Houston, TX, 1991. (distributed by COSMIC, NASA's Computer Software Management and Information Center, The University of Georgia, Computer Services Annex, Athens, GA 30602, Ph. (404)542-3265)

[3] Raju, I.S., "Computations of Stress Intensity for Flaws in Flat and Cylindrical Surfaces," Subcontractor Report to LESC P.O. 02N0140125-1, Analytical Services and Materials Inc., Hampton, VA, April 1991.

[4] Forman, R.G., Mettu, S.R., Shivakumar, V., "Fracture Mechanics Evaluation of Pressure Vessels and Pipes in Aerospace Applications," Proceedings of the ASME Pressure Vessels and Piping Conference, Eds. H.S. Mehta et. al., Fracture, Fatigue and Risk, PVP-Vol. 241, pp. 25–36, New Orleans, LA, 1992.

[5] Raju, I.S., and Newman, J.C., "Stress Intensity Factors for Internal and External Surface Cracks in Cylindrical Vessels," Journal of Pressure Vessel Technology, 104, 1982, pp. 293–298.

[6] Raju, I.S., Mettu, S.R., Shivakumar, V., "Stress Intensity Factor Solutions for Surface Cracks in Flat Plates Subjected to Nonuniform Stress," presented at the 24th National Symposium on Fracture Mechanics, Gatlinburg, TN, June 30 – July 2, 1992.

[7] Bueckner, H.F., "A Novel Principle for the Computation of Stress Intensity Factors," Z. Angew. Math. Mech., 50, 1970, pp. 129–146.

[8] Rice, J.R., "Some Remarks on Elastic Crack-tip Stress Field," Int. J. Solids Struct., 8, 1972, pp. 751–758.

[9] Shen, G., Glinka, G., "Determination of Weight Functions from Reference Stress Intensity Factors," Theoretical and Applied Fracture Mechanics, 15, 1991, pp. 237–245.

[10] Shen, G., Glinka, G., "Weight Functions for a Surface Semi-elliptical Crack in a Finite Thickness Plate," Theoretical and Applied Fracture Mechanics, 15, 1991, pp. 247–255.

U.S. Gov't

TABLE 1–*SIF Correction Factors F_p for Internal Cracks*

	$a/c = 0.2$					$a/c = 0.4$					$a/c = 1.0$				
$a/t \rightarrow$ 0	.2	.5	.8	1.0	0	.2	.5	.8	1.0	0	.2	.5	.8	1.0
R/t														
c-tip, Uniform Loading($n = 0$)														
1.0	0.608	0.615	0.871	1.554	2.277	0.740	0.745	0.916	1.334	1.752	1.044	1.080	1.116	1.132	1.131
2.0	0.600	0.614	0.817	1.300	1.783	0.730	0.760	0.919	1.231	1.519	1.132	1.113	1.155	1.286	1.416
4.0	0.577	0.606	0.797	1.201	1.586	0.737	0.770	0.924	1.219	1.487	1.119	1.128	1.191	1.316	1.428
10.0	0.579	0.607	0.791	1.179	1.548	0.733	0.777	0.936	1.219	1.469	1.114	1.140	1.219	1.348	1.456
300.0	0.582	0.613	0.790	1.148	1.482	0.721	0.782	0.946	1.201	1.413	1.133	1.154	1.239	1.389	1.520
c-tip, Linear Loading($n = 1.0$)															
1.0	0.083	0.085	0.171	0.363	0.544	0.112	0.119	0.181	0.307	0.421	0.169	0.182	0.200	0.218	0.229
2.0	0.078	0.083	0.150	0.291	0.421	0.072	0.122	0.197	0.271	0.317	0.192	0.190	0.207	0.247	0.285
4.0	0.070	0.079	0.141	0.262	0.370	0.110	0.123	0.174	0.263	0.339	0.188	0.194	0.214	0.248	0.277
10.0	0.070	0.079	0.138	0.253	0.356	0.109	0.125	0.176	0.259	0.328	0.187	0.197	0.221	0.255	0.282
300.0	0.068	0.081	0.138	0.239	0.328	0.103	0.127	0.180	0.253	0.310	0.189	0.201	0.227	0.265	0.294
a-tip, Uniform Loading($n = 0$)															
1.0	1.076	1.056	1.395	2.530	3.846	1.051	1.011	1.149	1.600	2.087	0.992	0.987	1.010	1.070	1.128
2.0	1.049	1.091	1.384	2.059	2.739	1.075	1.045	1.160	1.510	1.876	1.037	1.003	1.023	1.129	1.242
4.0	1.003	1.097	1.405	1.959	2.461	1.024	1.057	1.193	1.443	1.665	1.005	1.009	1.041	1.105	1.162
10.0	0.973	1.115	1.427	1.872	2.230	0.992	1.072	1.217	1.393	1.521	0.994	1.015	1.050	1.090	1.118
300.0	0.936	1.145	1.459	1.774	1.974	0.982	1.095	1.244	1.370	1.438	1.002	1.026	1.058	1.085	1.099
a-tip, Linear Loading($n = 1.0$)															
1.0	0.693	0.647	0.767	1.174	1.615	0.689	0.646	0.694	0.889	1.093	0.704	0.701	0.709	0.730	0.750
2.0	0.673	0.661	0.764	1.033	1.301	0.674	0.659	0.710	0.854	0.995	0.732	0.707	0.714	0.774	0.840
4.0	0.649	0.666	0.776	0.996	1.197	0.668	0.666	0.715	0.828	0.934	0.720	0.713	0.726	0.768	0.810
10.0	0.635	0.673	0.783	0.960	1.108	0.656	0.672	0.723	0.806	0.875	0.715	0.715	0.729	0.760	0.788
300.0	0.620	0.681	0.790	0.917	1.008	0.651	0.677	0.727	0.791	0.838	0.716	0.715	0.726	0.751	0.775

U.S. Gov't

TABLE 2–*SIF Correction Factors F_p for External Cracks*

	$a/c = 0.2$					$a/c = 0.4$					$a/c = 1.0$				
$a/t \rightarrow$ 0	.2	.5	.8	1.0	0	.2	.5	.8	1.0	0	.2	.5	.8	1.0	
R/t															
c-tip, Uniform Loading($n = 0$)															
1.0	0.755	0.594	0.648	1.293	2.129	0.889	0.809	0.934	1.492	2.143	1.148	1.202	1.354	1.594	1.796
2.0	0.720	0.611	0.693	1.207	1.826	0.817	0.796	0.959	1.425	1.915	1.152	1.185	1.318	1.560	1.775
4.0	0.589	0.612	0.786	1.160	1.517	0.754	0.793	0.994	1.400	1.781	1.127	1.163	1.286	1.498	1.681
10.0	0.598	0.612	0.806	1.262	1.715	0.750	0.788	0.984	1.378	1.747	1.123	1.156	1.266	1.453	1.613
300.0	0.582	0.613	0.790	1.148	1.482	0.721	0.782	0.946	1.201	1.413	1.133	1.154	1.239	1.389	1.520
c-tip, Linear Loading($n = 1.0$)															
1.0	0.153	0.076	0.089	0.271	0.481	0.170	0.132	0.170	0.329	0.497	0.202	0.214	0.256	0.327	0.387
2.0	0.121	0.079	0.105	0.245	0.395	0.140	0.130	0.182	0.315	0.443	0.196	0.209	0.250	0.315	0.370
4.0	0.073	0.080	0.134	0.242	0.339	0.118	0.130	0.195	0.318	0.427	0.189	0.204	0.243	0.302	0.350
10.0	0.078	0.080	0.142	0.277	0.402	0.114	0.128	0.192	0.309	0.411	0.188	0.202	0.236	0.286	0.326
300.0	0.068	0.081	0.138	0.239	0.328	0.103	0.127	0.180	0.253	0.310	0.189	0.201	0.227	0.265	0.294
a-tip, Uniform Loading($n = 0$)															
1.0	1.244	1.237	1.641	2.965	4.498	1.146	1.175	1.452	2.119	2.800	1.030	1.054	1.146	1.305	1.442
2.0	1.111	1.193	1.655	2.732	3.842	1.077	1.136	1.403	1.942	2.454	1.020	1.044	1.117	1.236	1.335
4.0	1.009	1.162	1.640	2.510	3.313	1.000	1.109	1.360	1.727	2.025	0.986	1.030	1.094	1.156	1.194
10.0	0.981	1.147	1.584	2.298	2.921	0.975	1.096	1.310	1.565	1.749	0.982	1.025	1.078	1.118	1.137
300.0	0.936	1.145	1.459	1.774	1.974	0.982	1.095	1.244	1.370	1.438	1.002	1.026	1.058	1.085	1.099
a-tip, Linear Loading($n = 1.0$)															
1.0	0.754	0.719	0.867	1.336	1.839	0.716	0.709	0.806	1.046	1.279	0.715	0.725	0.760	0.817	0.866
2.0	0.688	0.700	0.868	1.255	1.634	0.685	0.692	0.785	0.984	1.168	0.720	0.722	0.746	0.797	0.844
4.0	0.650	0.691	0.861	1.178	1.464	0.655	0.685	0.773	0.914	1.032	0.711	0.720	0.743	0.777	0.804
10.0	0.636	0.685	0.839	1.099	1.323	0.645	0.680	0.755	0.858	0.938	0.709	0.718	0.738	0.765	0.786
300.0	0.620	0.681	0.790	0.917	1.008	0.651	0.677	0.727	0.791	0.838	0.716	0.715	0.726	0.751	0.775

U.S. Gov't

TABLE 3–*SIF Correction Factors F_p for Internal Cracks*

	$a/c = 0.2$					$a/c = 0.4$					$a/c = 1.0$				
$a/t \rightarrow$ 0	.2	.5	.8	1.0	0	.2	.5	.8	1.0	0	.2	.5	.8	1.0
R/t														
c-tip, Quadratic Loading($n = 2.0$)														
1.0	0.023	0.027	0.069	0.155	0.233	0.035	0.041	0.073	0.132	0.183	0.064	0.067	0.078	0.095	0.110
2.0	0.021	0.025	0.058	0.123	0.180	0.044	0.043	0.064	0.114	0.161	0.070	0.071	0.080	0.098	0.115
4.0	0.015	0.023	0.054	0.108	0.154	0.033	0.042	0.068	0.109	0.143	0.068	0.072	0.082	0.097	0.109
10.0	0.016	0.023	0.052	0.104	0.149	0.032	0.043	0.069	0.106	0.135	0.068	0.074	0.085	0.099	0.109
300.0	0.015	0.024	0.051	0.096	0.134	0.031	0.045	0.071	0.102	0.126	0.068	0.076	0.088	0.103	0.113
c-tip, Cubic Loading($n = 3.0$)															
1.0	0.009	0.013	0.038	0.085	0.127	0.015	0.020	0.040	0.073	0.101	0.032	0.034	0.041	0.051	0.060
2.0	0.008	0.012	0.031	0.067	0.099	0.021	0.021	0.034	0.062	0.089	0.035	0.036	0.042	0.052	0.061
4.0	0.005	0.010	0.028	0.059	0.085	0.015	0.021	0.036	0.059	0.078	0.034	0.037	0.043	0.050	0.055
10.0	0.005	0.010	0.027	0.056	0.081	0.014	0.021	0.036	0.056	0.071	0.035	0.038	0.044	0.051	0.056
300.0	0.005	0.011	0.026	0.051	0.070	0.013	0.022	0.037	0.054	0.066	0.034	0.039	0.046	0.053	0.057
a-tip, Quadratic Loading($n = 2.0$)															
1.0	0.531	0.495	0.557	0.772	0.995	0.536	0.504	0.529	0.642	0.761	0.574	0.577	0.623	0.675	
2.0	0.519	0.502	0.556	0.708	0.858	0.527	0.511	0.536	0.623	0.710	0.594	0.577	0.580	0.619	0.661
4.0	0.511	0.511	0.567	0.692	0.808	0.528	0.520	0.545	0.614	0.681	0.597	0.588	0.594	0.623	0.653
10.0	0.499	0.514	0.571	0.671	0.757	0.520	0.523	0.549	0.601	0.647	0.590	0.588	0.596	0.618	0.639
300.0	0.486	0.514	0.569	0.641	0.696	0.512	0.520	0.546	0.585	0.618	0.585	0.581	0.586	0.604	0.622
a-tip, Cubic Loading($n = 3.0$)															
1.0	0.434	0.408	0.446	0.580	0.716	0.444	0.421	0.435	0.510	0.589	0.506	0.491	0.493	0.523	0.556
2.0	0.427	0.413	0.446	0.545	0.643	0.436	0.425	0.441	0.498	0.555	0.505	0.493	0.495	0.521	0.549
4.0	0.430	0.426	0.460	0.542	0.619	0.451	0.439	0.454	0.509	0.565	0.518	0.511	0.515	0.536	0.558
10.0	0.446	0.438	0.462	0.529	0.594	0.443	0.441	0.456	0.493	0.528	0.518	0.512	0.515	0.532	0.550
300.0	0.405	0.420	0.454	0.501	0.537	0.427	0.431	0.446	0.473	0.496	0.499	0.496	0.499	0.511	0.523

U.S. Gov't

TABLE 4–*SIF Correction Factors F_p for External Cracks*

	$a/c = 0.2$					$a/c = 0.4$					$a/c = 1.0$				
$a/t \rightarrow$ 0	.2	.5	.8	1.0	0	.2	.5	.8	1.0	0	.2	.5	.8	1.0	
R/t															
c-tip, Quadratic Loading($n = 2.0$)															
1.0	0.060	0.021	0.026	0.109	0.202	0.064	0.046	0.064	0.136	0.210	0.076	0.081	0.100	0.133	0.161
2.0	0.041	0.022	0.035	0.097	0.162	0.049	0.046	0.071	0.131	0.188	0.072	0.079	0.098	0.127	0.151
4.0	0.018	0.023	0.049	0.097	0.139	0.036	0.045	0.078	0.134	0.181	0.068	0.077	0.096	0.122	0.142
10.0	0.020	0.023	0.053	0.114	0.169	0.036	0.045	0.076	0.129	0.174	0.068	0.076	0.092	0.113	0.129
300.0	0.015	0.024	0.051	0.096	0.134	0.031	0.045	0.071	0.102	0.126	0.068	0.076	0.088	0.103	0.113
c-tip, Cubic Loading($n = 3.0$)															
1.0	0.032	0.009	0.011	0.058	0.110	0.032	0.023	0.033	0.073	0.114	0.039	0.042	0.053	0.071	0.087
2.0	0.020	0.010	0.017	0.051	0.086	0.023	0.022	0.037	0.071	0.102	0.036	0.041	0.052	0.068	0.080
4.0	0.006	0.010	0.025	0.051	0.073	0.017	0.022	0.041	0.073	0.100	0.034	0.040	0.051	0.064	0.073
10.0	0.007	0.010	0.028	0.062	0.092	0.017	0.022	0.040	0.070	0.095	0.034	0.039	0.048	0.059	0.067
300.0	0.005	0.011	0.026	0.051	0.070	0.013	0.022	0.037	0.054	0.066	0.034	0.039	0.046	0.053	0.057
a-tip, Quadratic Loading($n = 2.0$)															
1.0	0.564	0.536	0.615	0.858	1.107	0.546	0.539	0.589	0.714	0.833	0.577	0.586	0.606	0.634	0.657
2.0	0.522	0.524	0.614	0.817	1.009	0.528	0.528	0.576	0.682	0.780	0.585	0.584	0.597	0.625	0.652
4.0	0.507	0.524	0.613	0.782	0.932	0.518	0.530	0.575	0.653	0.720	0.589	0.591	0.603	0.625	0.644
10.0	0.501	0.521	0.600	0.739	0.859	0.516	0.528	0.565	0.625	0.675	0.588	0.590	0.600	0.619	0.636
300.0	0.486	0.514	0.569	0.641	0.696	0.512	0.520	0.546	0.585	0.618	0.585	0.581	0.586	0.604	0.622
a-tip, Cubic Loading($n = 3.0$)															
1.0	0.454	0.435	0.486	0.635	0.783	0.448	0.444	0.474	0.550	0.621	0.490	0.499	0.513	0.527	0.537
2.0	0.426	0.427	0.484	0.609	0.726	0.436	0.436	0.465	0.530	0.591	0.498	0.498	0.505	0.523	0.538
4.0	0.427	0.434	0.488	0.596	0.693	0.440	0.445	0.472	0.523	0.568	0.513	0.513	0.520	0.536	0.551
10.0	0.422	0.432	0.480	0.568	0.645	0.439	0.444	0.466	0.505	0.539	0.515	0.513	0.518	0.533	0.548
300.0	0.405	0.420	0.454	0.501	0.537	0.427	0.431	0.446	0.473	0.496	0.499	0.496	0.499	0.511	0.523

U.S. Gov't

TABLE 5–*SIF Correction Factors F_p for Internal Cracks*

	$a/c = 0.2$					$a/c = 0.4$					$a/c = 1.0$				
$a/t \rightarrow$ 0	.2	.5	.8	1.0	0	.2	.5	.8	1.0	0	.2	.5	.8	1.0	
R/t															
c-tip, Loading Power: $n = 0.5$															
1.0	0.195	0.195	0.333	0.664	0.989	0.247	0.253	0.349	0.560	0.757	0.369	0.370	0.395	0.451	0.501
2.0	0.187	0.193	0.301	0.540	0.766	0.273	0.259	0.325	0.503	0.677	0.390	0.385	0.410	0.476	0.540
300.0	0.173	0.191	0.284	0.459	0.616	0.233	0.269	0.355	0.481	0.581	0.389	0.404	0.448	0.516	0.573
c-tip, Loading Power: $n = 1.5$															
1.0	0.041	0.044	0.103	0.227	0.341	0.059	0.066	0.109	0.192	0.266	0.102	0.105	0.118	0.143	0.164
2.0	0.038	0.043	0.088	0.181	0.264	0.072	0.068	0.097	0.168	0.235	0.110	0.110	0.122	0.148	0.173
300.0	0.031	0.041	0.079	0.144	0.200	0.053	0.071	0.107	0.154	0.189	0.108	0.117	0.135	0.157	0.174
a-tip, Loading Power: $n = 0.5$															
1.0	0.830	0.788	0.975	1.606	2.311	0.821	0.774	0.850	1.128	1.424	0.846	0.807	0.819	0.920	1.031
2.0	0.808	0.808	0.970	1.368	1.766	0.820	0.793	0.862	1.076	1.293	0.845	0.816	0.827	0.904	0.989
300.0	0.734	0.840	1.011	1.198	1.325	0.771	0.821	0.901	0.987	1.044	0.823	0.828	0.845	0.874	0.898
a-tip, Loading Power: $n = 1.5$															
1.0	0.600	0.558	0.642	0.929	1.232	0.601	0.564	0.597	0.742	0.895	0.655	0.629	0.634	0.692	0.757
2.0	0.584	0.568	0.640	0.837	1.033	0.593	0.572	0.605	0.717	0.830	0.654	0.633	0.638	0.685	0.738
300.0	0.543	0.583	0.658	0.752	0.820	0.571	0.585	0.620	0.669	0.709	0.642	0.638	0.646	0.667	0.689

U.S. Gov't

TABLE 6–*SIF Correction Factors F_p for External Cracks*

	$a/c = 0.2$					$a/c = 0.4$					$a/c = 1.0$				
$a/t \rightarrow$ 0	.2	.5	.8	1.0	0	.2	.5	.8	1.0	0	.2	.5	.8	1.0	
R/t															
c-tip, Loading Power: $n = 0.5$															
1.0	0.297	0.182	0.206	0.519	0.893	0.336	0.278	0.342	0.615	0.911	0.404	0.427	0.499	0.618	0.719
2.0	0.257	0.188	0.232	0.475	0.746	0.290	0.275	0.359	0.587	0.812	0.399	0.418	0.486	0.600	0.697
300.0	0.173	0.191	0.284	0.459	0.616	0.233	0.269	0.355	0.481	0.581	0.389	0.404	0.448	0.516	0.573
c-tip, Loading Power: $n = 1.5$															
1.0	0.091	0.037	0.045	0.164	0.298	0.099	0.073	0.099	0.202	0.309	0.118	0.125	0.152	0.199	0.239
2.0	0.067	0.039	0.057	0.147	0.242	0.078	0.073	0.108	0.194	0.276	0.113	0.122	0.149	0.191	0.225
300.0	0.031	0.041	0.079	0.144	0.200	0.053	0.071	0.107	0.154	0.189	0.108	0.117	0.135	0.157	0.174
a-tip, Loading Power: $n = 0.5$															
1.0	0.923	0.894	1.122	1.852	2.667	0.868	0.869	1.021	1.392	1.760	0.830	0.844	0.896	0.985	1.062
2.0	0.835	0.867	1.126	1.725	2.327	0.824	0.844	0.990	1.295	1.580	0.831	0.838	0.877	0.951	1.015
300.0	0.734	0.840	1.011	1.198	1.325	0.771	0.821	0.901	0.987	1.044	0.823	0.828	0.845	0.874	0.898
a-tip, Loading Power: $n = 1.5$															
1.0	0.643	0.611	0.716	1.044	1.386	0.617	0.609	0.677	0.845	1.007	0.636	0.645	0.671	0.711	0.743
2.0	0.592	0.596	0.715	0.988	1.250	0.594	0.596	0.660	0.802	0.933	0.643	0.643	0.660	0.698	0.733
300.0	0.543	0.583	0.658	0.752	0.820	0.571	0.585	0.620	0.669	0.709	0.642	0.638	0.646	0.667	0.689

U.S. Gov't

TABLE 7–*SIF Correction Factors F_p for Internal Cracks*

	$a/c = 0.2$					$a/c = 0.4$					$a/c = 1.0$				
$a/t \rightarrow$ 0	.2	.5	.8	1.0	0	.2	.5	.8	1.0	0	.2	.5	.8	1.0	
R/t															
c-tip, Loading Power: $n = 2.5$															
1.0	0.013	0.018	0.050	0.113	0.169	0.022	0.028	0.053	0.096	0.133	0.044	0.047	0.055	0.068	0.079
2.0	0.012	0.017	0.042	0.089	0.131	0.030	0.029	0.045	0.082	0.117	0.048	0.049	0.056	0.070	0.082
300.0	0.008	0.015	0.036	0.068	0.095	0.019	0.030	0.050	0.073	0.089	0.047	0.053	0.062	0.072	0.078
c-tip, Loading Power: $n = 3.5$															
1.0	0.006	0.009	0.029	0.067	0.099	0.011	0.015	0.031	0.057	0.079	0.024	0.026	0.032	0.040	0.047
2.0	0.005	0.009	0.024	0.052	0.077	0.016	0.016	0.026	0.049	0.069	0.027	0.028	0.032	0.040	0.047
300.0	0.003	0.008	0.020	0.039	0.054	0.009	0.017	0.029	0.042	0.051	0.025	0.030	0.036	0.041	0.043
a-tip, Loading Power: $n = 2.5$															
1.0	0.478	0.447	0.495	0.662	0.833	0.485	0.458	0.477	0.568	0.664	0.547	0.529	0.532	0.569	0.610
2.0	0.469	0.453	0.494	0.615	0.735	0.477	0.463	0.483	0.553	0.623	0.546	0.532	0.534	0.565	0.600
300.0	0.442	0.462	0.504	0.562	0.606	0.465	0.471	0.490	0.523	0.550	0.538	0.535	0.539	0.554	0.569
a-tip, Loading Power: $n = 3.5$															
1.0	0.398	0.376	0.407	0.516	0.627	0.408	0.389	0.401	0.462	0.528	0.470	0.458	0.459	0.483	0.510
2.0	0.393	0.380	0.407	0.489	0.570	0.401	0.392	0.406	0.453	0.499	0.469	0.460	0.461	0.482	0.504
300.0	0.374	0.386	0.413	0.452	0.482	0.394	0.397	0.409	0.431	0.450	0.464	0.462	0.464	0.473	0.483

U.S. Gov't

TABLE 8–*SIF Correction Factors F_p for External Cracks*

	$a/c = 0.2$					$a/c = 0.4$					$a/c = 1.0$				
$a/t \rightarrow$ 0	.2	.5	.8	1.0	0	.2	.5	.8	1.0	0	.2	.5	.8	1.0	
R/t															
c-tip, Loading Power: $n = 2.5$															
1.0	0.043	0.013	0.017	0.077	0.146	0.044	0.031	0.044	0.097	0.151	0.053	0.057	0.071	0.095	0.115
2.0	0.028	0.014	0.023	0.068	0.116	0.033	0.031	0.050	0.094	0.136	0.050	0.055	0.070	0.091	0.107
300.0	0.008	0.015	0.036	0.068	0.095	0.019	0.030	0.050	0.073	0.089	0.047	0.053	0.062	0.072	0.078
c-tip, Loading Power: $n = 3.5$															
1.0	0.024	0.007	0.008	0.044	0.085	0.025	0.017	0.025	0.056	0.088	0.030	0.032	0.041	0.055	0.068
2.0	0.015	0.007	0.012	0.039	0.067	0.017	0.017	0.029	0.055	0.080	0.027	0.031	0.040	0.052	0.062
300.0	0.003	0.008	0.020	0.039	0.054	0.009	0.017	0.029	0.042	0.051	0.025	0.030	0.036	0.041	0.043
a-tip, Loading Power: $n = 2.5$															
1.0	0.503	0.480	0.542	0.730	0.918	0.492	0.486	0.524	0.620	0.712	0.530	0.539	0.555	0.575	0.590
2.0	0.469	0.470	0.540	0.698	0.845	0.477	0.477	0.513	0.596	0.672	0.538	0.537	0.547	0.569	0.590
300.0	0.442	0.462	0.504	0.562	0.606	0.465	0.471	0.490	0.523	0.550	0.538	0.535	0.539	0.554	0.569
a-tip, Loading Power:$n = 3.5$															
1.0	0.414	0.399	0.441	0.561	0.680	0.411	0.408	0.433	0.494	0.551	0.456	0.465	0.476	0.486	0.491
2.0	0.390	0.391	0.438	0.540	0.634	0.402	0.401	0.425	0.478	0.527	0.463	0.464	0.470	0.483	0.494
300.0	0.374	0.386	0.413	0.452	0.482	0.394	0.397	0.409	0.431	0.450	0.464	0.462	0.464	0.473	0.483

U.S. Gov't

TABLE 9 – *SIF Correction Factors F_0 for Internal Cracks*

	$a/c = 0.2$					$a/c = 0.4$					$a/c = 0.6$					$a/c = 0.8$					$a/c = 1.0$				
$a/t \rightarrow$	0	.2	.5	.8	1.0	0	.2	.5	.8	1.0	0	.2	.5	.8	1.0	0	.2	.5	.8	1.0	0	.2	.5	.8	1.0
R/t																									
c-tip, Uniform Loading																									
1.0	0.580	0.593	0.610	0.846	1.117	0.630	0.650	0.665	0.841	1.041	0.670	0.688	0.702	0.831	0.976	0.695	0.709	0.722	0.817	0.919	0.700	0.713	0.726	0.796	0.872
2.0	0.600	0.617	0.671	0.824	0.975	0.660	0.669	0.714	0.837	0.956	0.695	0.703	0.741	0.838	0.930	0.715	0.721	0.752	0.828	0.898	0.710	0.722	0.747	0.806	0.860
4.0	0.613	0.633	0.726	0.898	1.049	0.664	0.681	0.756	0.894	1.014	0.698	0.712	0.772	0.880	0.974	0.716	0.727	0.774	0.858	0.930	0.718	0.727	0.762	0.827	0.883
10.0	0.591	0.644	0.785	1.000	1.178	0.651	0.689	0.797	0.967	1.108	0.692	0.718	0.799	0.930	1.041	0.714	0.732	0.791	0.891	0.975	0.717	0.730	0.774	0.849	0.913
300.0	0.538	0.583	0.747	1.075	1.398	0.601	0.679	0.818	1.023	1.199	0.668	0.722	0.829	0.969	1.074	0.700	0.739	0.817	0.919	0.996	0.726	0.736	0.785	0.878	0.960
c-tip, Bending Loading																									
1.0	0.337	0.265	0.111	0.080	0.050	0.358	0.308	0.216	0.150	0.120	0.370	0.338	0.293	0.253	0.230	0.375	0.355	0.340	0.343	0.354	0.371	0.360	0.359	0.378	0.400
2.0	0.400	0.403	0.410	0.420	0.430	0.430	0.443	0.450	0.465	0.493	0.460	0.470	0.482	0.520	0.559	0.480	0.485	0.503	0.548	0.590	0.482	0.486	0.505	0.547	0.587
4.0	0.498	0.510	0.569	0.678	0.775	0.539	0.550	0.602	0.698	0.782	0.567	0.577	0.622	0.704	0.775	0.581	0.590	0.628	0.696	0.756	0.583	0.590	0.620	0.675	0.723
10.0	0.544	0.595	0.722	0.915	1.072	0.605	0.637	0.732	0.888	1.019	0.646	0.664	0.734	0.858	0.965	0.668	0.677	0.728	0.824	0.909	0.670	0.675	0.713	0.786	0.851
300.0	0.538	0.583	0.747	1.075	1.398	0.601	0.679	0.818	1.023	1.199	0.668	0.722	0.829	0.969	1.074	0.700	0.739	0.817	0.919	0.996	0.726	0.736	0.785	0.878	0.960
a-tip, Uniform Loading																									
1.0	0.960	0.987	1.064	1.665	2.406	0.875	0.888	0.944	1.360	1.857	0.795	0.799	0.841	1.119	1.437	0.720	0.721	0.754	0.941	1.146	0.650	0.653	0.684	0.823	0.969
2.0	0.990	1.022	1.093	1.380	1.685	0.900	0.911	0.961	1.163	1.377	0.800	0.813	0.847	0.985	1.130	0.710	0.726	0.751	0.846	0.943	0.620	0.652	0.674	0.745	0.815
4.0	1.031	1.045	1.141	1.332	1.504	0.920	0.926	0.991	1.123	1.243	0.819	0.821	0.862	0.951	1.031	0.729	0.729	0.756	0.814	0.868	0.650	0.652	0.672	0.713	0.751
10.0	0.983	1.059	1.189	1.337	1.440	0.888	0.936	1.020	1.120	1.192	0.800	0.827	0.878	0.941	0.989	0.718	0.732	0.761	0.801	0.831	0.642	0.651	0.671	0.697	0.717
300.0	1.059	1.090	1.384	1.682	1.881	0.948	0.951	1.079	1.188	1.251	0.792	0.832	0.888	0.940	0.971	0.720	0.733	0.754	0.777	0.792	0.642	0.656	0.675	0.691	0.700
a-tip, Bending Loading																									
1.0	0.520	0.545	0.659	1.074	1.523	0.470	0.493	0.597	0.919	1.254	0.430	0.446	0.542	0.792	1.039	0.385	0.405	0.494	0.693	0.879	0.350	0.368	0.454	0.621	0.771
2.0	0.700	0.719	0.821	1.088	1.352	0.630	0.643	0.728	0.935	1.135	0.560	0.575	0.648	0.808	0.957	0.503	0.515	0.579	0.706	0.819	0.448	0.463	0.523	0.629	0.720
4.0	0.839	0.865	0.974	1.173	1.347	0.748	0.767	0.849	0.997	1.126	0.666	0.681	0.743	0.852	0.946	0.592	0.606	0.654	0.735	0.805	0.528	0.542	0.583	0.648	0.702
10.0	0.902	0.985	1.120	1.267	1.366	0.822	0.871	0.959	1.064	1.141	0.744	0.770	0.824	0.897	0.954	0.669	0.682	0.715	0.765	0.806	0.597	0.607	0.631	0.667	0.695
300.0	1.059	1.090	1.384	1.682	1.881	0.948	0.951	1.079	1.188	1.251	0.792	0.832	0.888	0.940	0.971	0.720	0.733	0.754	0.777	0.792	0.642	0.656	0.675	0.691	0.700

TABLE 10 - SIF Correction Factors F_0 for External Cracks

	$a/c = 0.2$					$a/c = 0.4$					$a/c = 0.6$					$a/c = 0.8$					$a/c = 1.0$				
$a/t \rightarrow$	0	.2	.5	.8	1.0	0	.2	.5	.8	1.0	0	.2	.5	.8	1.0	0	.2	.5	.8	1.0	0	.2	.5	.8	1.0
R/t																									
c-tip, Uniform Loading																									
1.0	0.590	0.672	0.893	1.249	1.552	0.664	0.713	0.871	1.138	1.368	0.712	0.739	0.846	1.039	1.209	0.734	0.747	0.818	0.954	1.075	0.731	0.739	0.788	0.882	0.966
2.0	0.560	0.660	0.876	1.177	1.416	0.643	0.706	0.859	1.086	1.271	0.699	0.734	0.838	1.006	1.148	0.727	0.744	0.814	0.938	1.046	0.728	0.737	0.787	0.881	0.964
4.0	0.540	0.653	0.873	1.162	1.383	0.630	0.701	0.858	1.081	1.257	0.691	0.731	0.839	1.006	1.145	0.722	0.742	0.815	0.940	1.046	0.725	0.735	0.786	0.880	0.962
10.0	0.542	0.646	0.867	1.172	1.414	0.630	0.697	0.855	1.087	1.275	0.689	0.728	0.838	1.010	1.153	0.720	0.741	0.815	0.941	1.049	0.722	0.734	0.785	0.879	0.961
300.0	0.538	0.583	0.747	1.075	1.398	0.601	0.679	0.818	1.023	1.199	0.668	0.722	0.829	0.969	1.074	0.700	0.739	0.817	0.919	0.996	0.726	0.736	0.785	0.878	0.960
c-tip, Bending Loading																									
1.0	0.592	0.643	0.742	0.870	0.967	0.659	0.690	0.761	0.861	0.940	0.704	0.720	0.768	0.844	0.908	0.727	0.731	0.760	0.819	0.871	0.729	0.724	0.740	0.785	0.829
2.0	0.552	0.645	0.798	0.972	1.092	0.632	0.691	0.801	0.939	1.040	0.687	0.720	0.795	0.902	0.987	0.716	0.731	0.780	0.863	0.932	0.720	0.724	0.757	0.820	0.876
4.0	0.545	0.645	0.835	1.075	1.254	0.624	0.690	0.827	1.014	1.158	0.678	0.717	0.814	0.956	1.069	0.706	0.728	0.794	0.899	0.987	0.710	0.722	0.767	0.845	0.912
10.0	0.524	0.633	0.850	1.136	1.357	0.612	0.684	0.840	1.057	1.229	0.672	0.715	0.823	0.984	1.115	0.703	0.727	0.801	0.918	1.016	0.705	0.721	0.772	0.859	0.932
300.0	0.538	0.583	0.747	1.075	1.398	0.601	0.679	0.818	1.023	1.199	0.668	0.722	0.829	0.969	1.074	0.700	0.739	0.817	0.919	0.996	0.726	0.736	0.785	0.878	0.960
a-tip, Uniform Loading																									
1.0	1.140	1.189	1.469	2.179	2.898	1.000	1.019	1.188	1.583	1.969	0.860	0.872	0.960	1.140	1.303	0.737	0.748	0.785	0.847	0.899	0.644	0.647	0.660	0.685	0.708
2.0	1.126	1.167	1.370	1.759	2.112	0.975	1.005	1.132	1.362	1.564	0.844	0.865	0.935	1.051	1.149	0.733	0.746	0.780	0.827	0.866	0.640	0.648	0.663	0.683	0.698
4.0	1.099	1.157	1.320	1.576	1.790	0.959	0.999	1.103	1.260	1.388	0.835	0.862	0.923	1.006	1.072	0.728	0.746	0.777	0.815	0.843	0.637	0.649	0.666	0.683	0.693
10.0	1.079	1.146	1.284	1.470	1.615	0.945	0.993	1.083	1.198	1.284	0.827	0.859	0.914	0.977	1.020	0.724	0.745	0.776	0.806	0.825	0.636	0.650	0.668	0.684	0.693
300.0	1.059	1.090	1.384	1.682	1.881	0.948	0.951	1.079	1.188	1.251	0.792	0.832	0.888	0.940	0.971	0.720	0.733	0.754	0.777	0.792	0.642	0.656	0.675	0.691	0.700
a-tip, Bending Loading																									
1.0	1.110	1.124	1.252	1.676	2.120	0.945	0.958	1.008	1.207	1.419	0.850	0.816	0.810	0.857	0.914	0.729	0.697	0.656	0.624	0.608	0.641	0.601	0.545	0.495	0.466
2.0	1.115	1.121	1.236	1.487	1.721	0.966	0.964	1.018	1.144	1.263	0.836	0.827	0.837	0.876	0.915	0.726	0.711	0.694	0.681	0.675	0.635	0.615	0.585	0.554	0.534
4.0	1.097	1.124	1.242	1.429	1.586	0.949	0.969	1.035	1.138	1.223	0.822	0.834	0.863	0.905	0.937	0.716	0.720	0.725	0.728	0.730	0.630	0.625	0.619	0.605	0.593
10.0	1.042	1.117	1.248	1.403	1.514	0.918	0.969	1.051	1.142	1.205	0.808	0.839	0.885	0.930	0.959	0.709	0.727	0.750	0.767	0.775	0.623	0.634	0.645	0.649	0.649
300.0	1.059	1.090	1.384	1.682	1.881	0.948	0.951	1.079	1.188	1.251	0.792	0.832	0.888	0.940	0.971	0.720	0.733	0.754	0.777	0.792	0.642	0.656	0.675	0.691	0.700

Figure Captions

Figure 1.- Geometry of Crack Cases in NASA/FLAGRO: SC02, SC03.

Figure 2.- Geometry of Crack Cases in NASA/FLAGRO: SC04, SC05.

Figure 3.- Power-type Stress Distributions, $n = 0, 1, 2, 3$.

Figure 4.- A Sample Finite Element Mesh for SC05

Figure 5.- Two Reference Stresses used in Weight Function for SC02, SC04.

Figure 6.- SICF : FEM and WF Solutions for SC04, Internal, c-tip, R/t=1, $n = 0, 1, 2, 3$.

Figure 7.- SICF : FEM and WF Solutions for SC04, Internal, a-tip, R/t=1, $n = 0, 1, 2, 3$.

Figure 8.- SICF : FEM and WF Solutions for SC04, Internal, c-tip, R/t=2, $n = 0, 1, 2, 3$.

Figure 9.- SICF : FEM and WF Solutions for SC04, Internal, a-tip, R/t=2, $n = 0, 1, 2, 3$.

Figure 10.- SICF : FEM and WF Solutions for SC04, External, c-tip, R/t=1, $n = 0, 1, 2, 3$.

Figure 11.- SICF : FEM and WF Solutions for SC04, External, a-tip, R/t=1, $n = 0, 1, 2, 3$.

Figure 12.- SICF : FEM and WF Solutions for SC04, External, c-tip, R/t=2, $n = 0, 1, 2, 3$.

Figure 13.- SICF : FEM and WF Solutions for SC04, External, a-tip, R/t=2, $n = 0, 1, 2, 3$.

U.S. Gov't

SC02

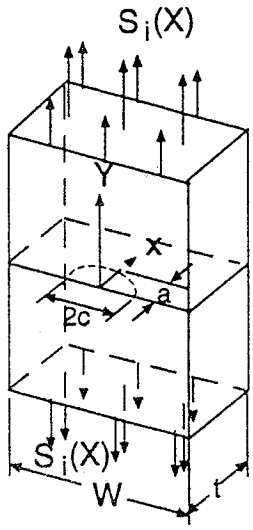

$i = 0, 1, 2, 3$

$$0 < \frac{2c}{W} \leq 1$$

SC03

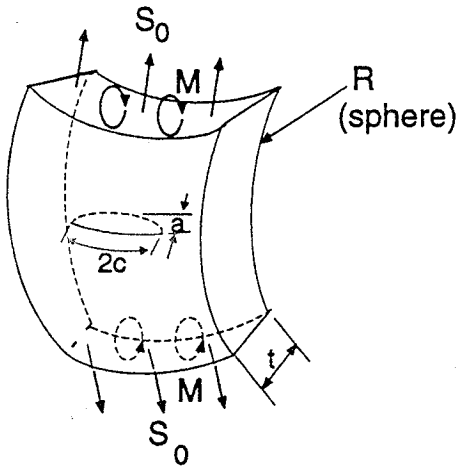

$$S_1 = \frac{6\,M}{W\,t^2}, \quad S_2 = p$$

internal or external crack

U.S. Gov't

Figure 1.- Geometry of Crack Cases in NASA/FLAGRO: SC02, SC03.

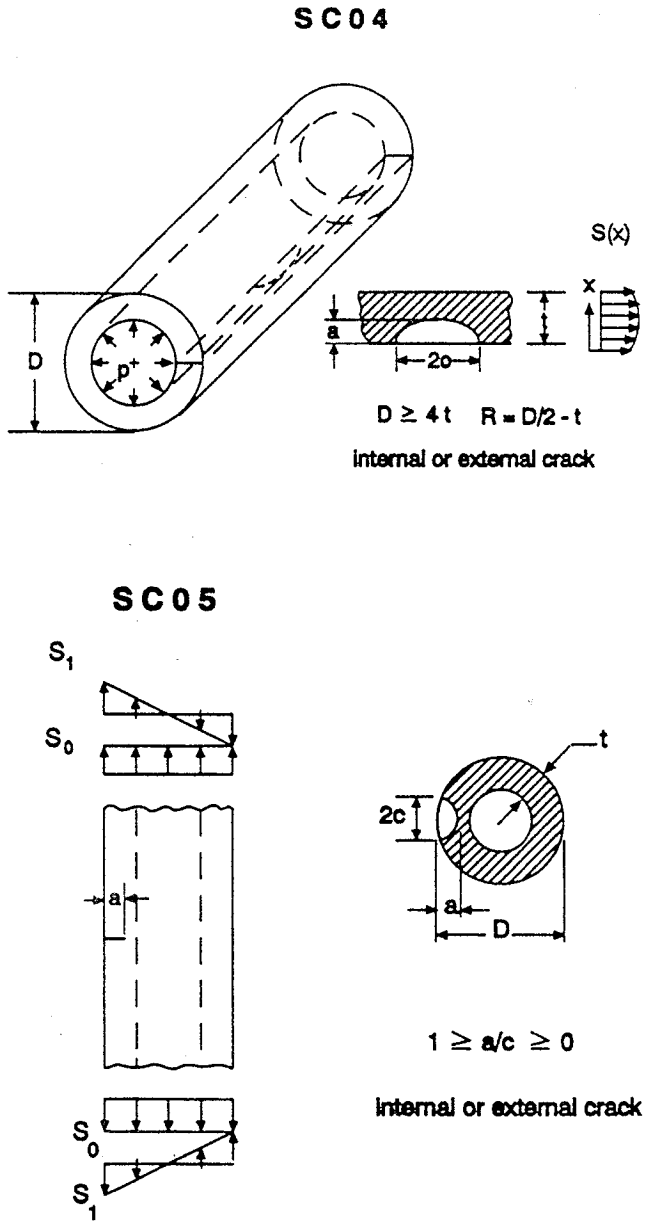

Figure 2.- Geometry of Crack Cases in NASA/FLAGRO: SC04, SC05.

U.S. Gov't

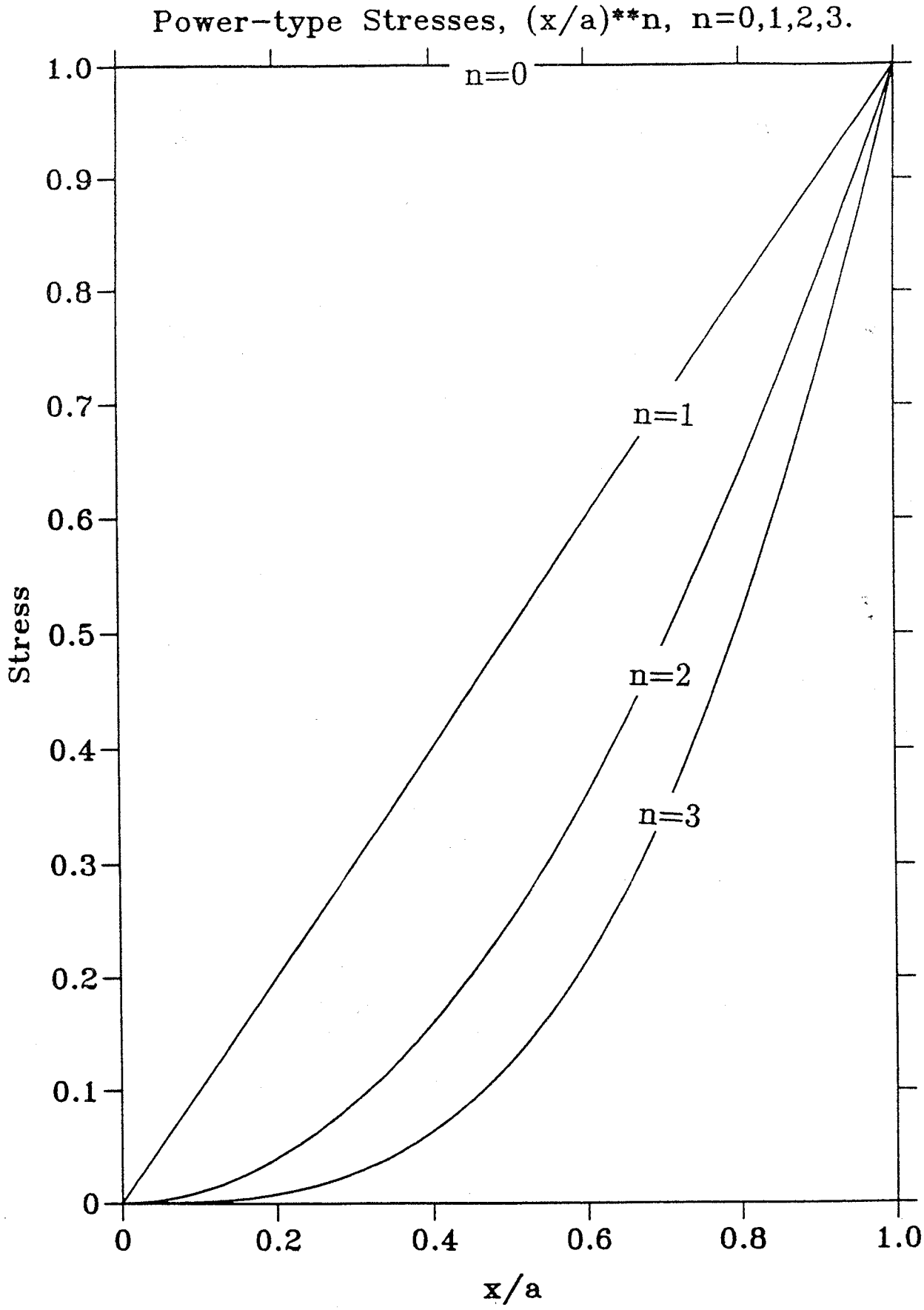

Fig. 3.-Power-type Stess Distributions, $n = 0, 1, 2, 3$.

U.S. Gov't

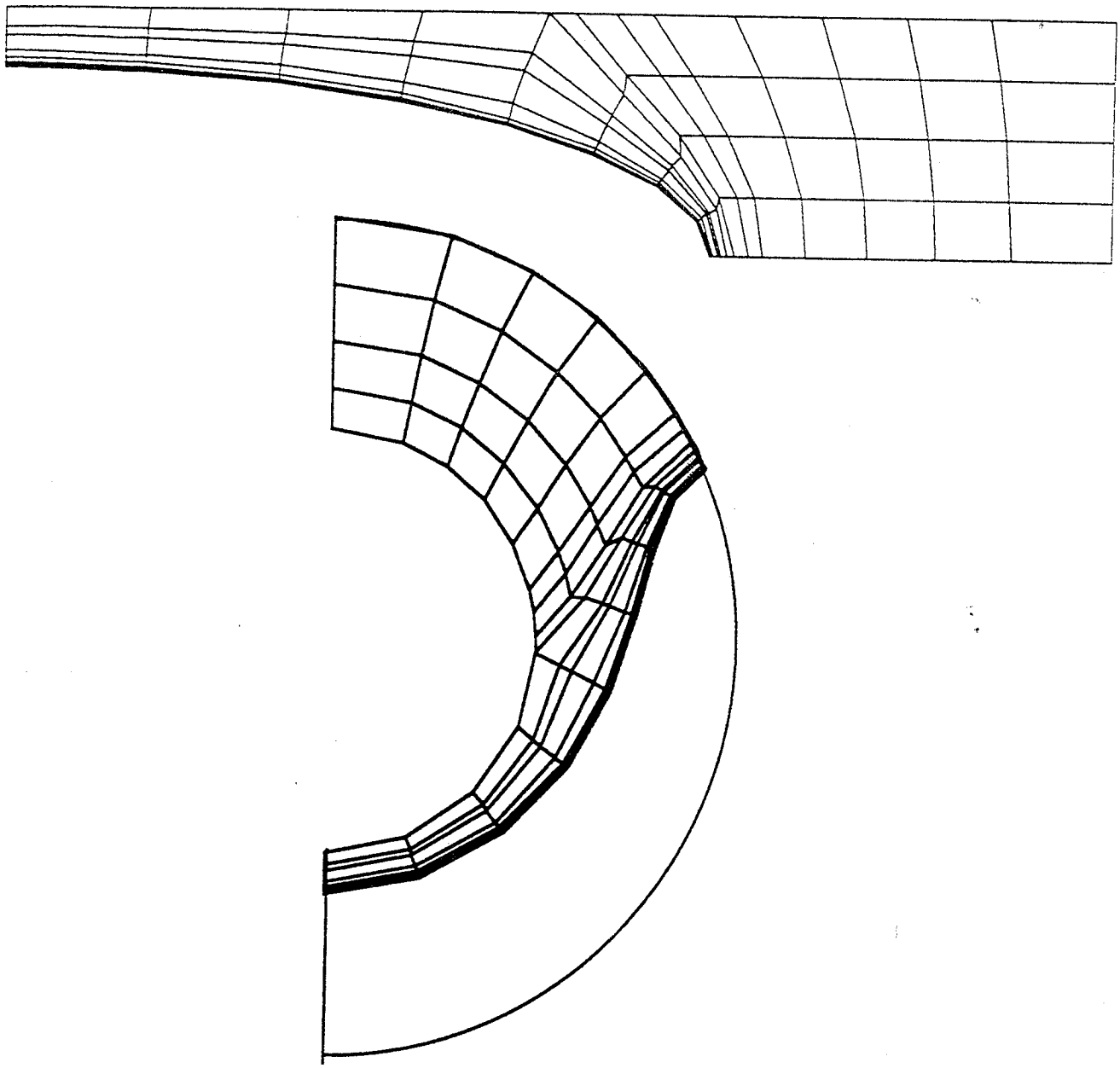

Figure 4.- A Sample Finite Element Mesh for SC05

U.S. Gov't

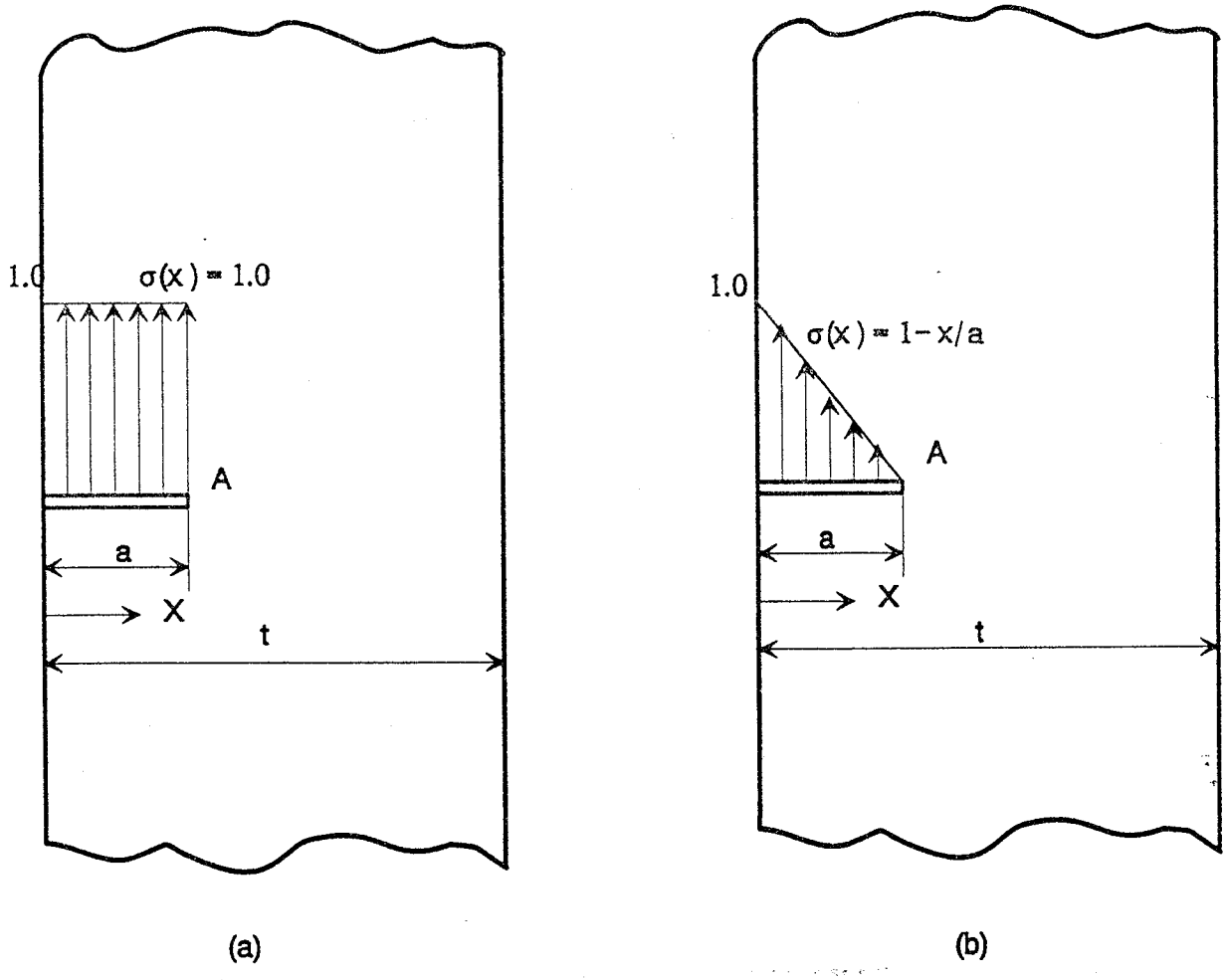

Fig. 5.- Two Reference Stresses used in the Weight-Function Method

U.S. Gov't

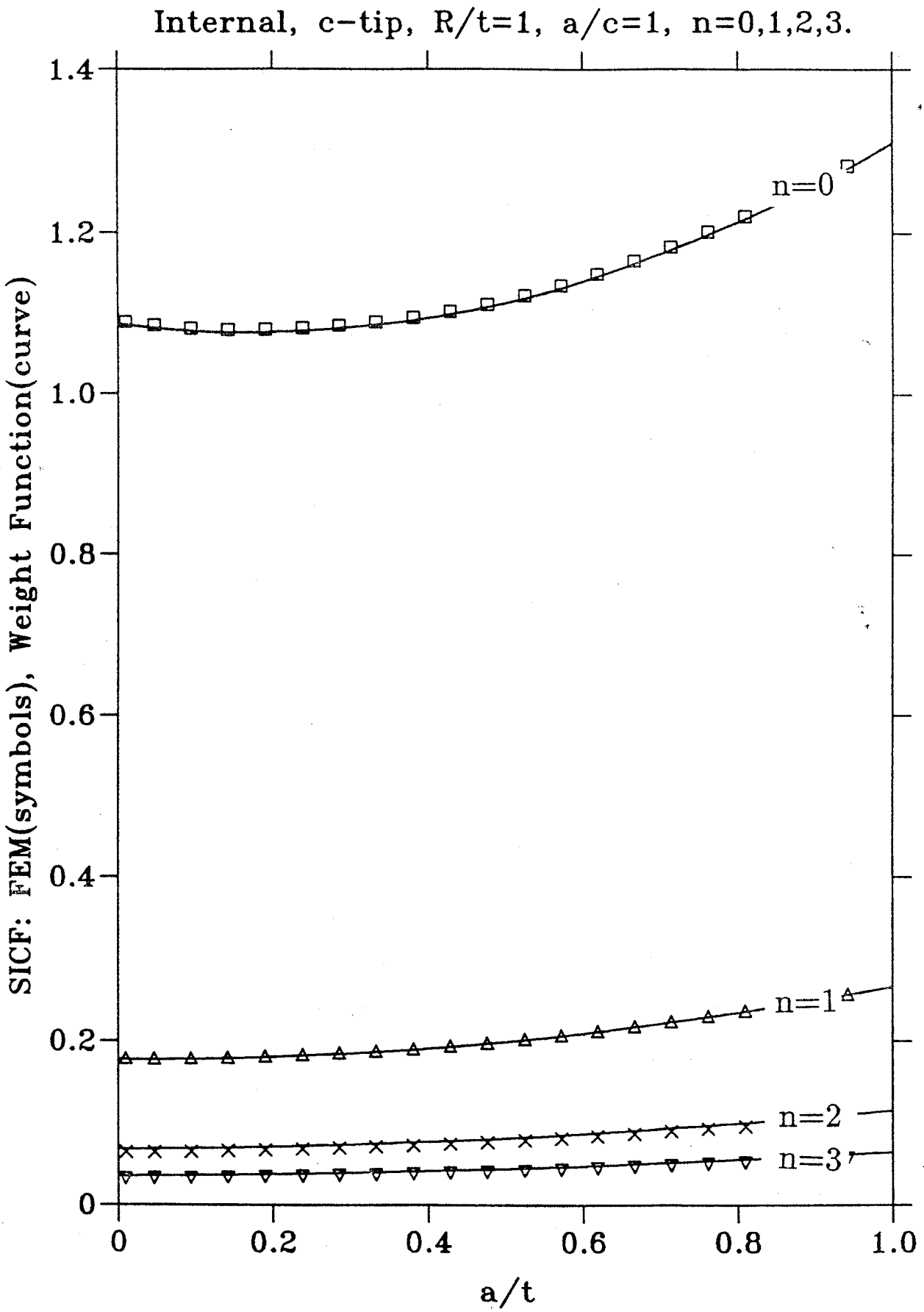

Figure 6.- SICF : FEM and WF Solutions for SC04, Internal, c-tip, R/t=1, $n = 0, 1, 2, 3$.

U.S. Gov't

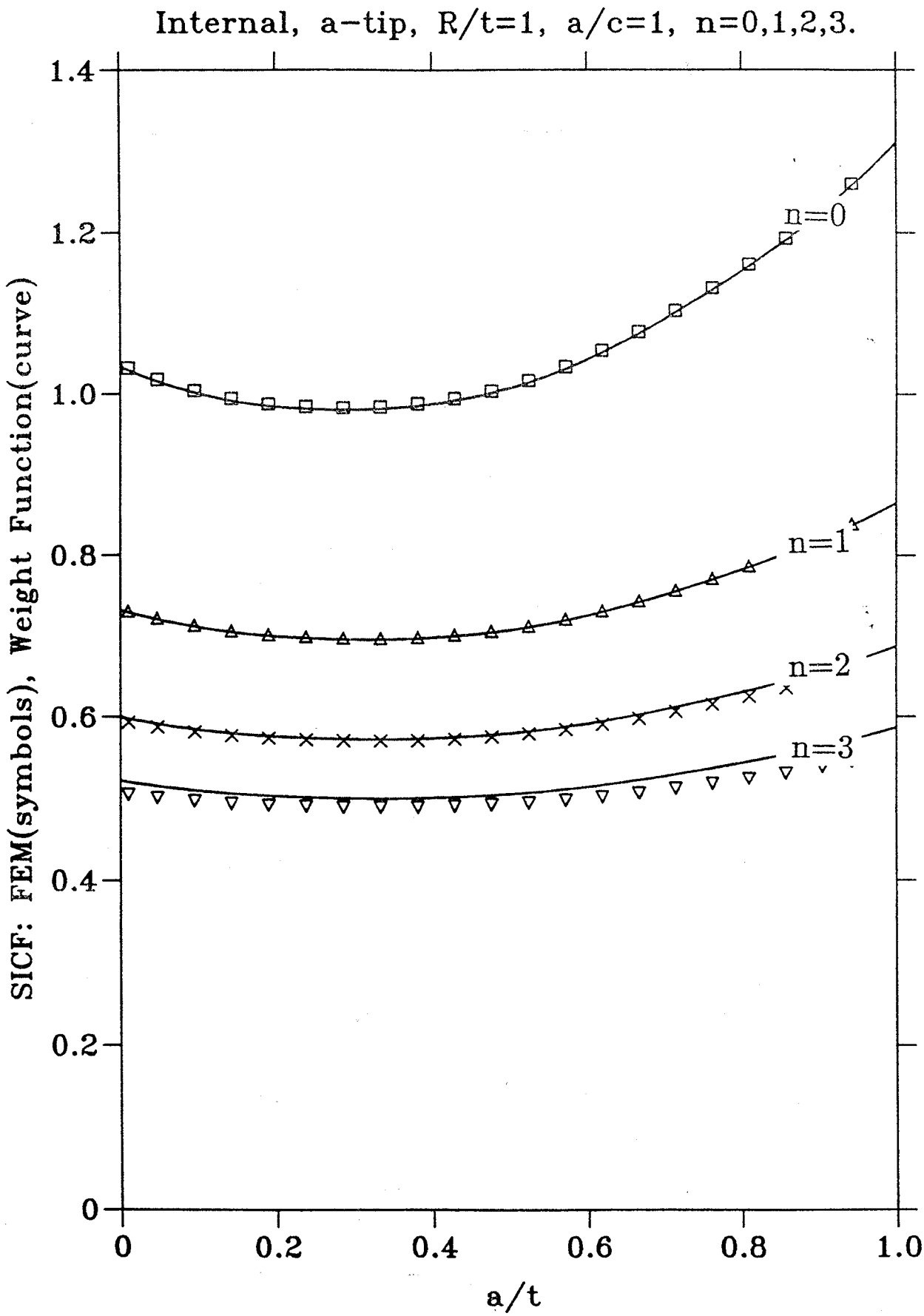

Figure 7.- SICF : FEM and WF Solutions for SC04, Internal, a-tip, R/t=1, $n = 0, 1, 2, 3$.

U.S. Gov't

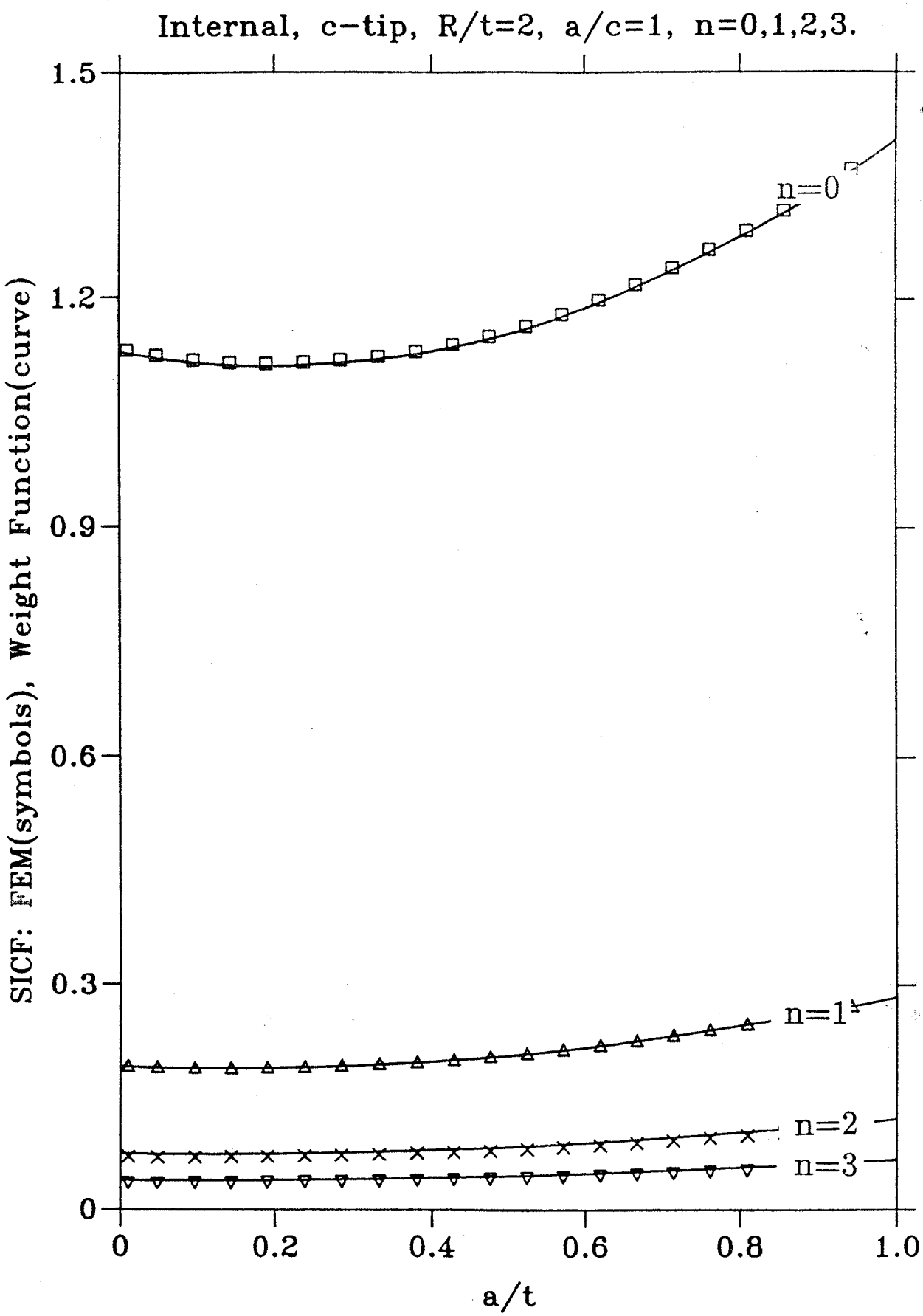

Figure 8.- SICF : FEM and WF Solutions for SC04, Internal, c-tip, R/t=2, $n = 0, 1, 2, 3$.

U.S. Gov't

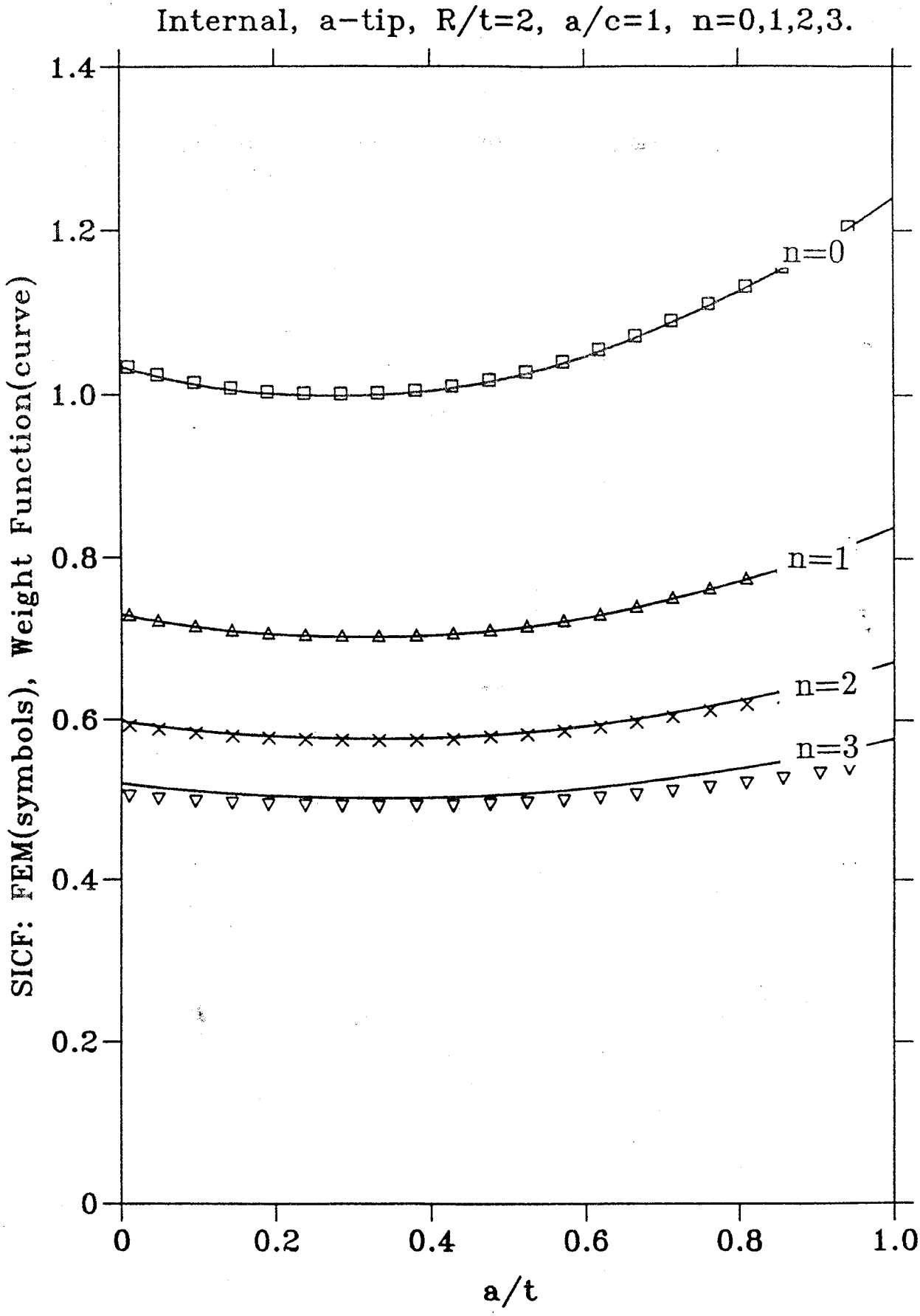

Figure 9.- SICF : FEM and WF Solutions for SC04, Internal, a-tip, R/t=2, $n = 0, 1, 2, 3$.

U.S. Gov't

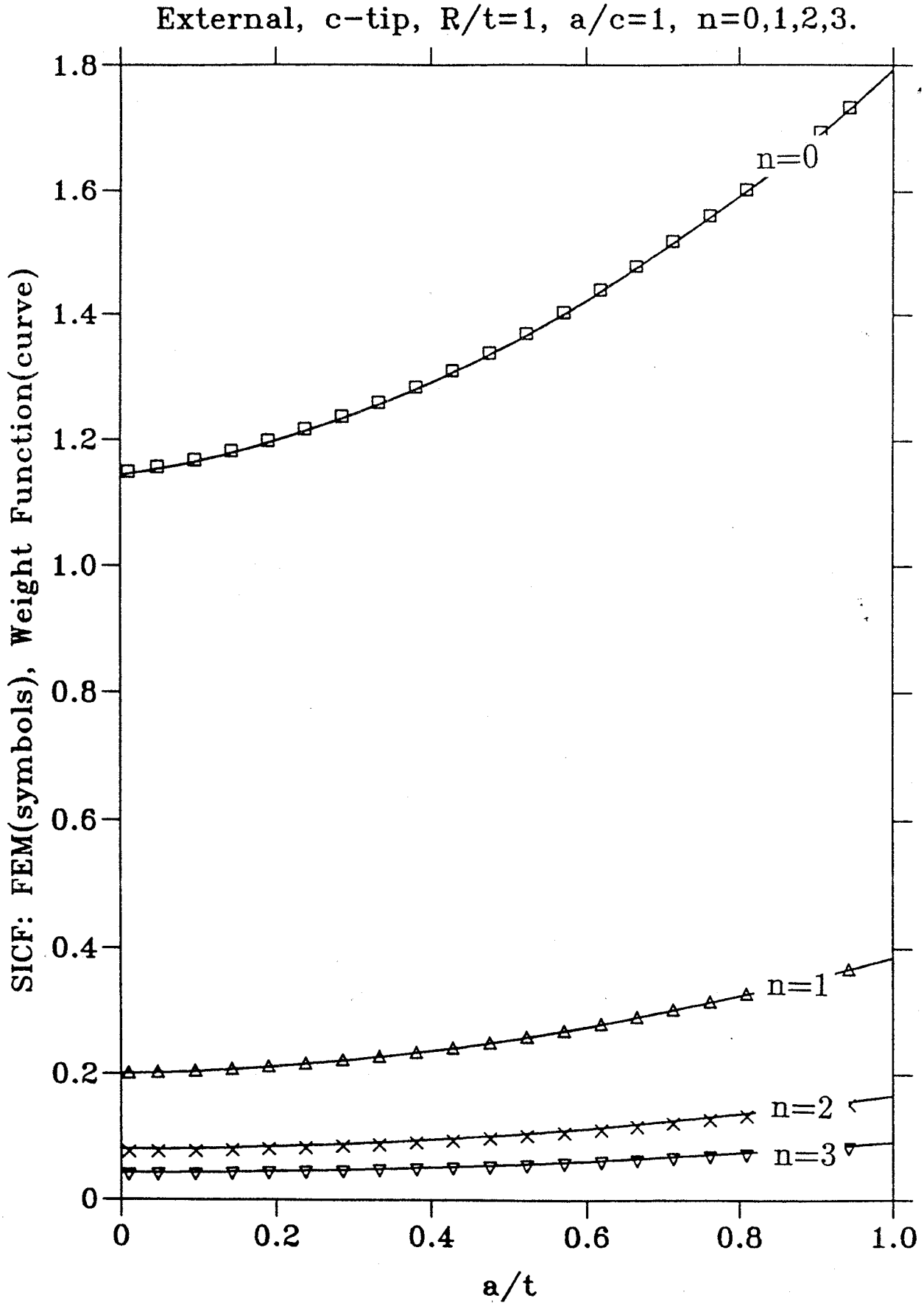

Figure 10.- SICF : FEM and WF Solutions for SC04, External, c-tip, R/t=1, $n = 0, 1, 2, 3$.

U.S. Gov't

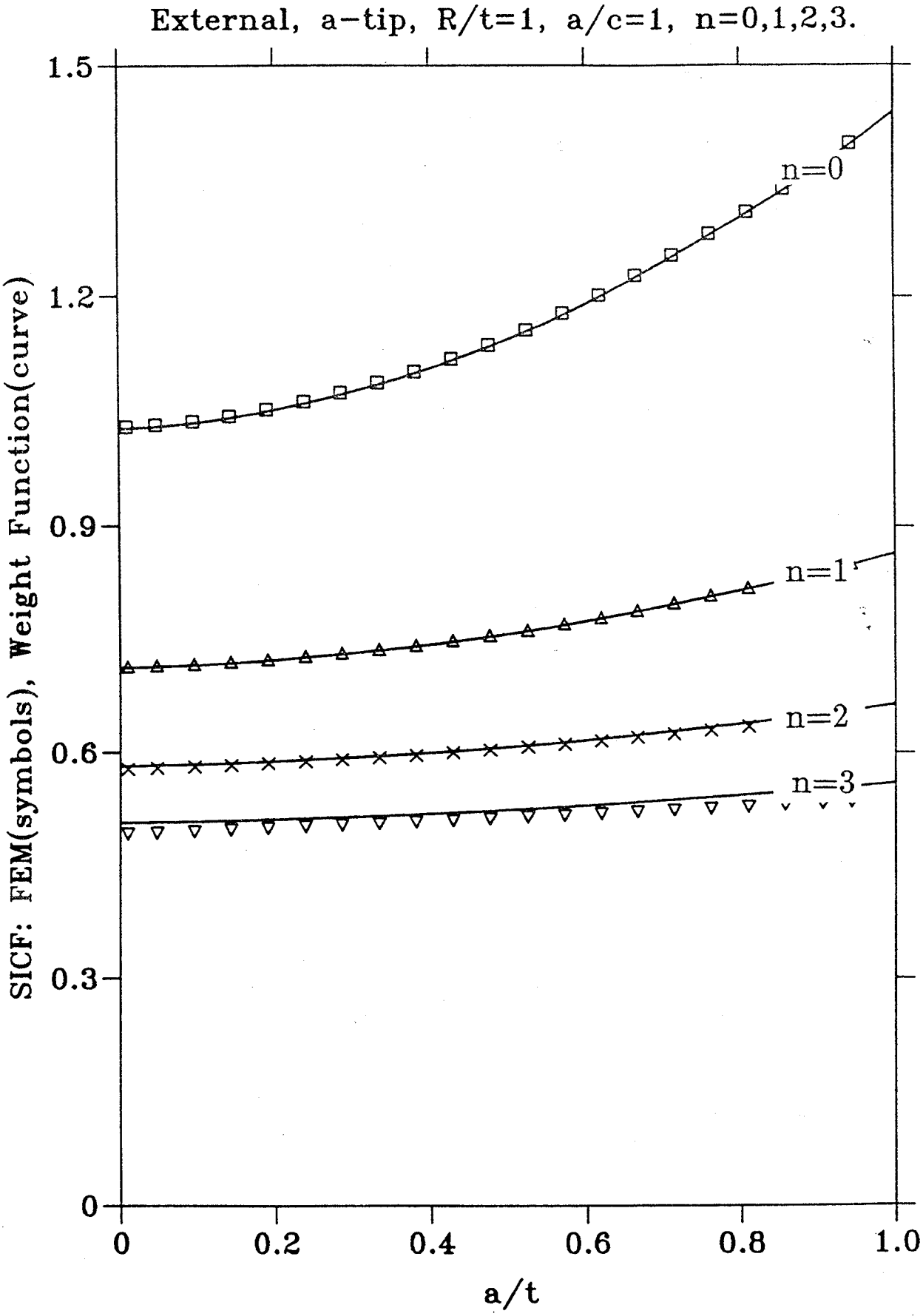

Figure 11.- SICF : FEM and WF Solutions for SC04, External, a-tip, R/t=1, $n = 0, 1, 2, 3$.

U.S. Gov't

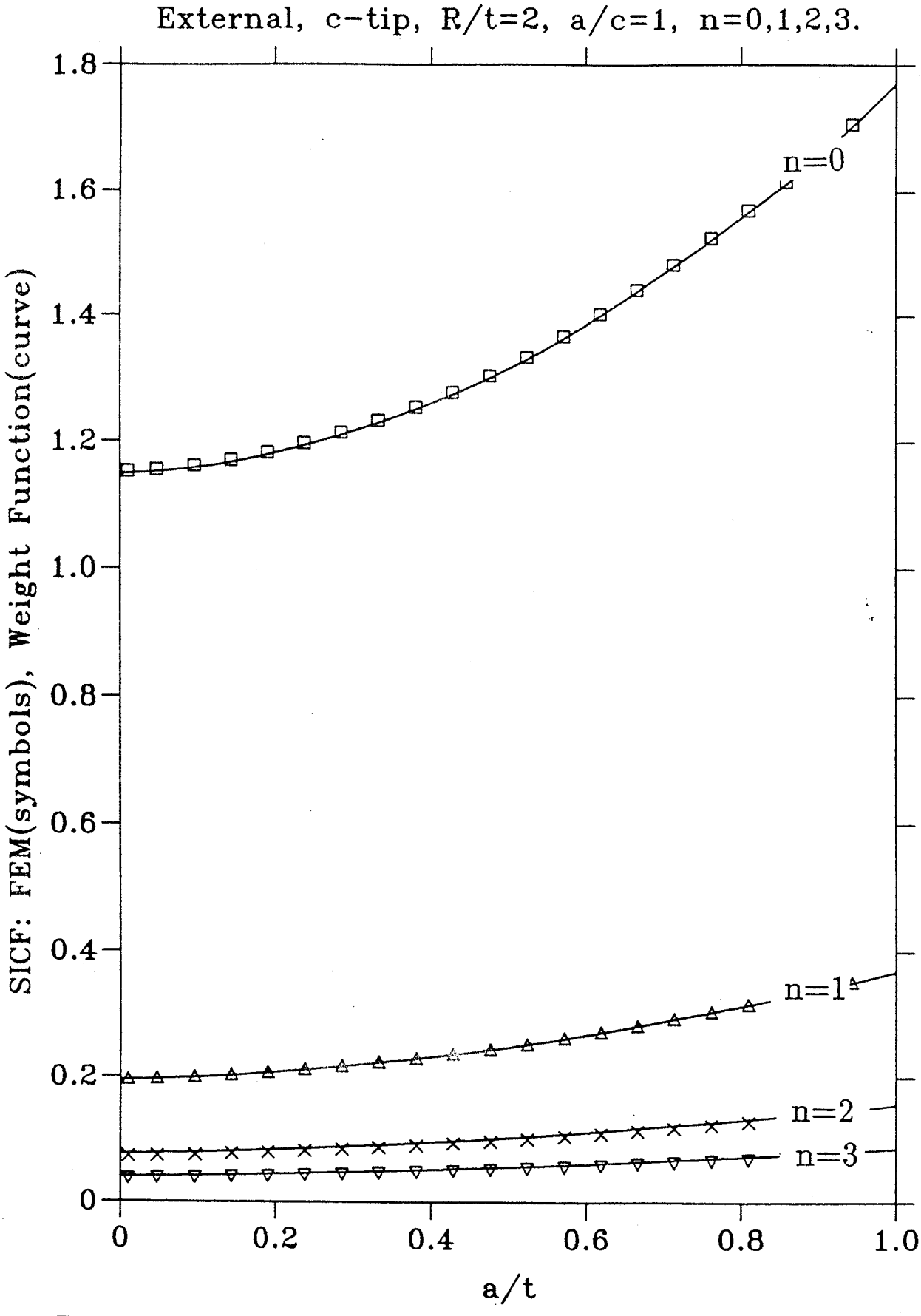

Figure 12.- SICF : FEM and WF Solutions for SC04, External, c-tip, R/t=2, $n = 0, 1, 2, 3$.

U.S. Gov't

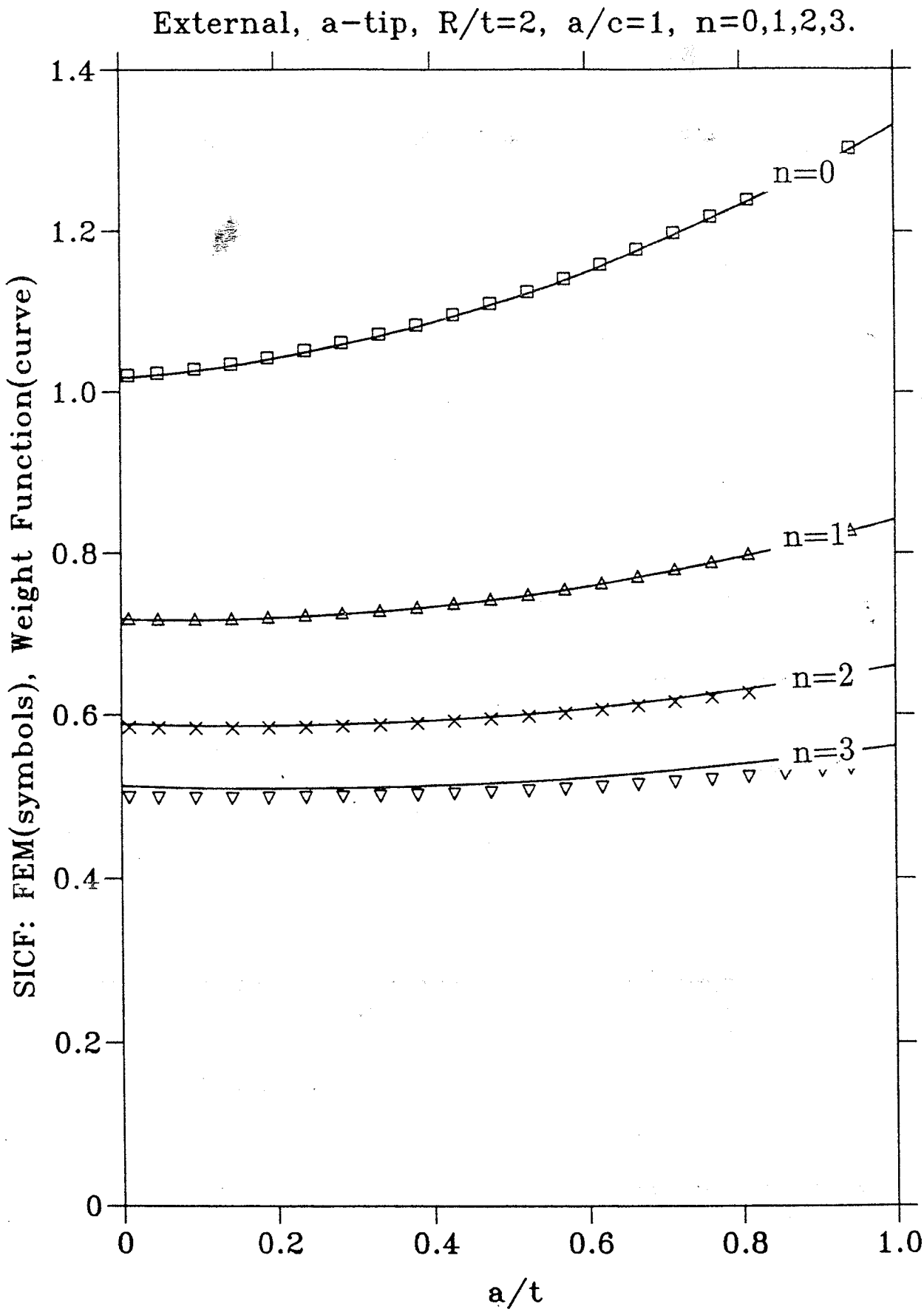

Figure 13.- SICF : FEM and WF Solutions for SC04, External, a-tip, R/t=2, $n = 0, 1, 2, 3$.

U.S. Gov't

The Flight Crew Support Division desires to strengthen its cognitive human factors expertise in the future. To this end, the Co-Operative Engineering Office is requested to assist the Division by recruiting and hiring candidates
with an interest in this area. Our need for Co-Ops with this background will
be on-going over the indefinite future. Applicable topics of interest might include the following:

- quantitative measurement of cognitive human performance during space operations
- evaluation of the ideal functional allocation between humans and automation
in space operations
- quantitative determination of optimal space vehicle displays and controls
- definition of improved operator interfaces to reduce crew training

As we strengthen the discipline, we hope to focus on applied human factors and
not theoretical research. We prefer individuals who have a specific interest
in cognitive human factors but also are operationally oriented. In essence, individuals who have an interest in space operations and wish to apply cognitive human factors principles to improve it.

The Division POC for this effort will be Ron Farris at 713/483-0881.

U.S. Gov't